Authors' reply to referee comments RC3 of the paper egusphere-2025-2903 entitled "Simulating liquid water distribution at the pore scale in snow: water retention curves and effective transport properties" by Bouvet et al.

We thank very much Reviewer 3 for the comments. Please find below our point-by-point replies in blue color.

The study addresses the spatial distribution of liquid water in different snow types and estimates its effect on various transport properties. The authors analyzed in detail 34 scanned dry snow samples and presented the results on water distribution not only in the main text but also in a well-organized and complete Supplementary Information folder (SI). This was well-appreciated and made it very easy (and interesting) to scrutinize the results of the study. Considering that experimental data on liquid water distribution at the pore scale of snow are rare, the authors based their analysis on numerical experiments. This strategy relies on evidence that the computed properties are reasonable and in agreement with experimental findings. More specifically, to trust the outcome of the numerical experiments, I would expect that (i) the capacity of the model is shown for a very few experimental cases (see a proposal below) and that the (ii) general trends are in good agreement with experimental studies. This proof is missing here, and I have some doubts regarding the results of the numerical experiments as I explain below.

We modified the manuscript substantially according to the reviewer comments. Concerning point (i), improvements have been made on the evaluation of our simulations of WRCs. Additional comparisons to experimental studies from the literature have been included, so that, to the best of our knowledge, all the data available in the literature are now included in the paper. Concerning point (ii), the discussion about the agreement of our simulations against experimental data has been revised and includes new elements. The limitations of our study are now stated in a dedicated section in the revised paper. The description of our improvement, especially regarding points (i) and (ii), is provided below in the corresponding reviewer comment.

Questions on the shape of the wetting curve

Typically, the shapes of the wetting and drainage curves are similar with a shift of the drainage curve to higher (absolute) capillary pressure values. This would be manifested in similar values of the parameter "n" for wetting and drying and in higher "alpha" values for the wetting curves (with "alpha" and "n" as shape parameters of the van Genuchten model to fit the relationship between water content and capillary pressure). While the study shows the expected correlation between the "alpha" values (with alpha_wetting 1.3 alpha_drainage according to the data in the SI), the values of "n" are very different from the expectations, with more or less constant value "n" for all wetting curves (3 to 6) that differs from the drainage curve with values ranging from 5 to 20 (average 10). Such a clear mismatch of the shapes of the wetting and drainage curves is unusual and also contradicts the experimental outcome presented in Table 1 of Adachi et al. (2020) that reported very similar values of "n" for wetting and drying curves.
In short, I don't trust the shape of the wetting curve with such smooth shape (different from drainage curve) and converging to the porosity. I would expect a large amount of entrapped air with water saturation values considerably smaller than the porosity.

Two elements of the simulated WRCs are pointed out in the above comment: the shape of the WRCs for imbibition compared to drainage, and the fact that the WRCs converge to the porosity.

Regarding the shape of our simulated WRCs in imbibition and drainage, we obtain smoother inflexions of the WRCs in imbibition than in drainage (sharper inflexions), which translates to lower n values for imbibition than for drainage; in addition, n values vary little for imbibition (range from 3 to 6) while they are more scattered for drainage (range from 5 to 20). In both cases, n values show no correlation with ρ/d. These findings are not consistent with the measurements of Adachi et al. (2020), as described by the reviewer. To further compare our results, we included additional comparisons in the revised version of the manuscript, shown in Figure 1: the studies of Katsushima et al. (2020) and Lombardo et al. (2025) provide n values for snow from drainage experiments and imbibition experiments, respectively. In contrast with Adachi et al. (2020), which showed n values similar for drainage and imbibition and in good agreement with the regression of Yamaguchi et al. (2012) (i.e. well correlated with ρ/d), these studies provide scattered values, ranging from 3 to 18 for the wetting process in Lombardo et al. (2025) and from 9 to 14 for the drainage in Katsushima et al. (2020). As in our data, these values are not correlated with ρ/d.

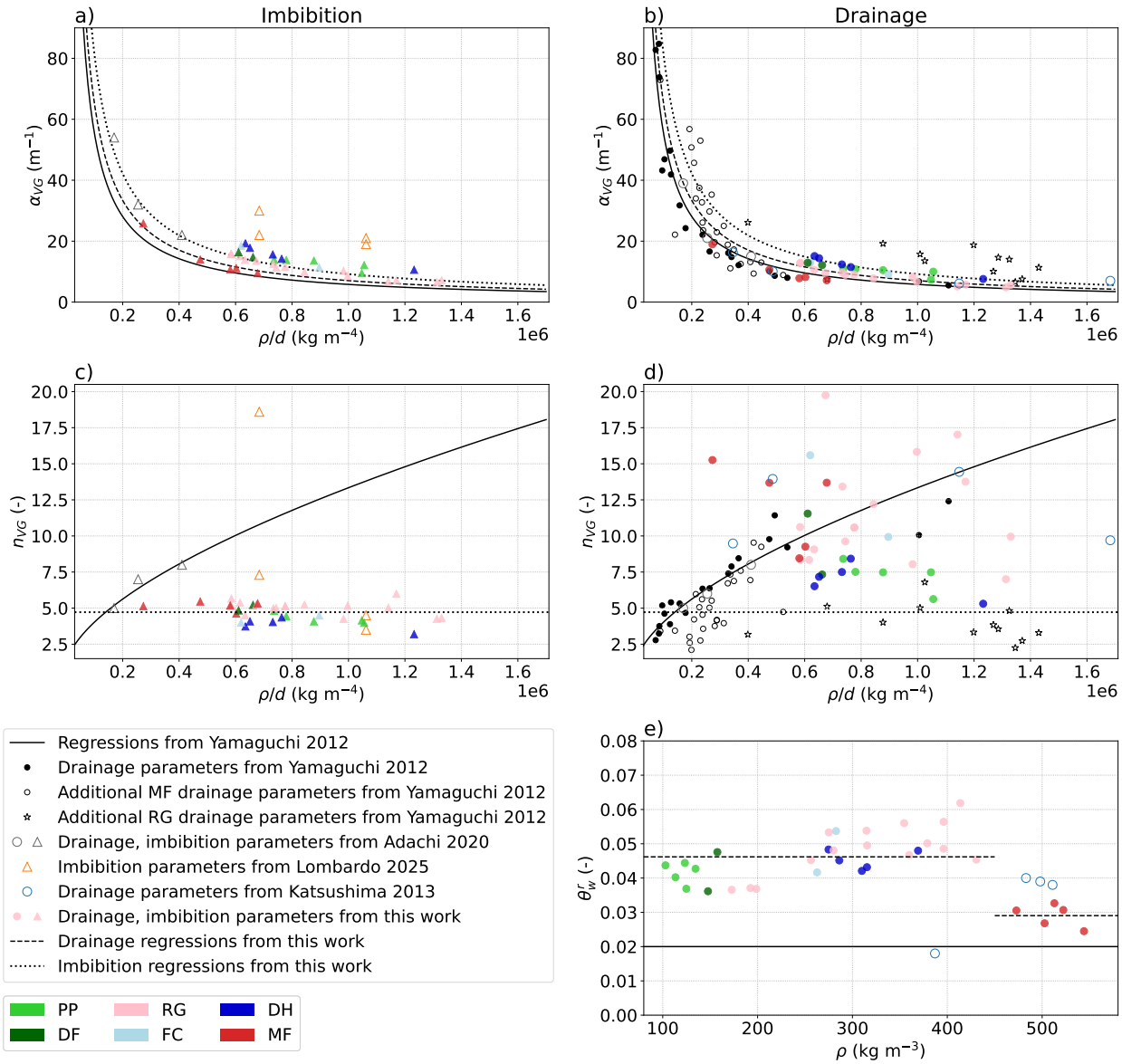

Figure 1. a) α_{vg}, b) n_{vg} and c) θ_w^r parameters of the VG model as a function of ρ/d or ρ for imbibition and drainage. The regressions of Yamaguchi et al. (2012) are shown by black lines, the values used to deduct those regressions are shown by black disks ("S-samples", composed of refrozen MF - see Yamaguchi et al. (2012)). The additional drainage measurements from Yamaguchi et al. (2012) are shown by circles (MF samples) and stars (RG samples). Measurements from Adachi et al. (2020) are shown by empty gray markers. Measurements from Lombardo et al. (2025) and Katsushima et al. (2013) are shown by empty orange triangles and blue circles. From this work, parameters from imbibition and drainage simulations are shown by colored disks and triangles, respectively, the colors showing the snow types. The proposed regressions based on our simulated data are shown by dashed and dotted lines (see Table 2).

This seems to indicate a more complex picture of the behavior of n than in the data of Adachi et al. (2012), and we can not invalidate the n values from our simulated WRCs. Moreover, different n values for imbibition and drainage was also reported

by Ahrenholz et al. (2008) for sand (Tableau D1, Fig. 3 and 4 in their paper): performing a cycle of drainage - wetting - re-drainage, they obtained n values of 11.4, 14.4, and 8.0 for the experiment referred as 'column 1' and 10.9, 4.9, and 8.7 for the experiment referred as 'column 2'.

In the revised version, the above considerations have been included. A discussion concerning the shape of our simulated WRCs and resulting n values is provided, including the comparison to the literature values. These modifications are found in Section 3.1.3 "Analysis of the VG parameters" (paragraph "n parameter") and in Figure 7 of the revised manuscript.

Regarding the second point of the reviewer's comment, the saturated water content θ_w^s equals the porosity in all our simulations. Indeed, we computed a primary imbibition curve assuming that there is no air (the non-wetting phase NWP) residuals, as in the Mercury Injection Capillary Pressure (MICP) experiments. This is a simplification of the process that occurs in nature, as in reality, residual air likely exists. We chose to do this simplification because the amount of air residual in the structure given by the Pore Morphology Method may depend significantly on the chosen boundary conditions on the four sides of the volume that are not connected to the wetting phase (WP) and NWP reservoirs. In Vogel et al. (2005), impervious boundary conditions are applied, whereas other conditions, such as symmetry, displaced fluid outlet, or invading fluid inlet, can also be applied (Berg et al., 2016). These boundary conditions may lead to different values of the NWP (air) residuals during the imbibition process, since these residuals can be trapped or not at the boundary. Testing that, we indeed obtained large discrepancies in the residual air content depending on the applied boundary conditions. The maximum water saturation (θ_w^s) may range from 45% to 90% of the porosity. These effects of the boundary conditions on θ_w^s also concern other methods to describe two-phase flows in 3D images and has been little discussed in the literature, to the best of our knowledge, except in (Galindo-Torres et al., 2016; Zhang et al., 2025) in the case of lattice Boltzmann simulations. This discrepancy was not, or to a much lesser extent, found in the residual of liquid water. Next, we looked at the literature on the residual air content in snow, we found θ_w^s values from measurements ranging from 0.6ϕ to 0.9ϕ (Yamaguchi et al., 2012; Katsushima et al., 2013; Adachi et al., 2020), with potentially large uncertainties linked to the experimental challenge of filling a snow column to its maximum, as already highlighted for other porous media (e.g., Clayton, 1999; Cho et al., 2022). Yamaguchi et al. (2012) suggested using a unique, fixed value of 0.9 ϕ for snow, when using the VG model, which seems rather arbitrary. Finally, we tested the impact of the residual air content on the shape parameters of the VG model: even with θ_w^s as low as 0.6ϕ, the difference in terms of VG parameters is mainly visible for α_{vg}, with differences around 10% of the value with $\theta_w^s = \phi$. This was also reported in the experiments of Likos et al. (2014) and Farooq et al. (2024), which showed that having θ_w^s smaller than ϕ generally implies greater α_{VG} values, but has no significant impact on the n_{VG} values. To conclude, for all the above reasons, we decided to simulate complete wetting so that $\theta_w^s = \phi$, while addressing the associated sources of error, and we encourage future studies to examine this question.

In the revised version, we improved the description of the simulation to clarify that no residual air was simulated during wetting (Section 2.3). We added a description on the impact of the $\theta_w^s = \phi$ simplification on our findings, in Section 3.1.3 'Analysis of the VG parameters' and in the new Section 'Main limitation' in the revised version.

Application of morphological pore network model (PNM)

I had good experience with the application of morphological pore network models (MPN) for the simulation of drainage processes in porous media, because it is controlled by the size distribution of the pore throats controlling the air invasion. The simulation of the wetting process, however, using spherical structural elements in the MPN, can be more critical: see Figures 5 and 6 in Ahrenholz et al. (2008) - you cited that study - and the sensitivity of the wetting curve with respect to the structural element. See the (i) large fractions of entrapped air in these figures and (ii) the similar shapes of wetting and drainage curves; these results are quite different compared to your findings shown for example in your Figure 4b (and in the data shown in the SI). I am puzzled by the text on lines 138-140: "For imbibition, the simulation starts with the 3D image of dry snow. A minimum pore radius is defined according to Eq. (5), which then increases step by step. At each time step, a pore is filled with liquid water if (i) the pore radius is below the minimum pore radius, and (ii) the liquid water phase is connected to the liquid water reservoir." Such a description is notcomplete -> the air phase must be continuous as well; it can occur that the invading water encloses air bubbles and then the air must stay entrapped. Was this ignored in this model?

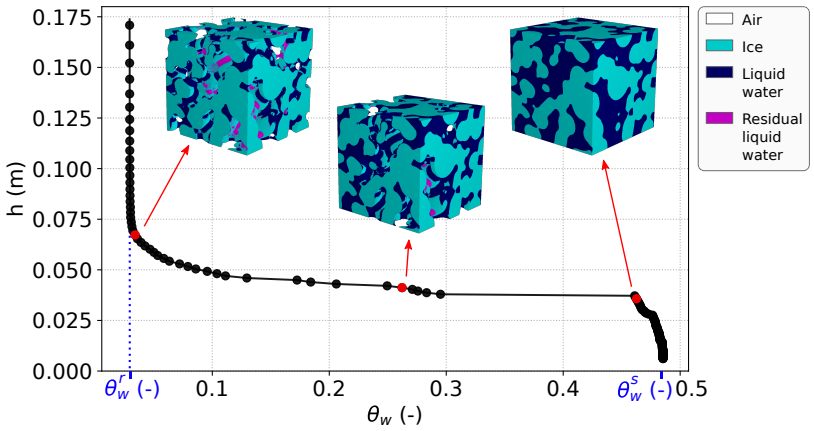

Figure 2. Example of a water retention curve estimated from a drainage simulation on a 3D tomographic snow sample of melt forms. The simulated 3D water distribution in the pores is shown at 3 different stages.

We agree with the reviewer. Air bubbles can be entrapped by the water during the imbibition process. As described in the previous comment, a complete imbibition process was simulated, and no residual air was computed. In the revised version, the description of the pore morphology method was substantially modified and includes all the above considerations (in the introduction and Section 2.3)

I'm also confused by the insets in Figure 2 that show the fluid distribution during the drainage process. The shape of the interface between water and air does not show the expected curvature 'with an air sphere invading the water filled pore space'.

We agree with the reviewer: the water menisci in Figure 2 did have a curvature in the wrong direction. This error was only made when plotting this particular example and not for the simulations. We changed Figure 2 accordingly, using the correct properties for a subsample of the image NH5. The corrected figure is presented here in Figure 2.

Thermal conductivity

The simulated thermal conductivity is a linear function of the water saturation. This linear relationship is unusual compared to findings for example in soils. In analogy to soils, I would assume that there is a fast increase in thermal conductivity with "the addition of a small amount of water" connecting the ice particles at the dry end. How can this strong linear relationship be explained? And what is with the case of theta=0 (after removal of the residual water)? Is there still a linear relationship between thermal conductivity and water content?

The thermal conductivity of water is four times less than the thermal conductivity of ice. Heat is thus conducted mostly through the ice skeleton. The dry snow thermal conductivity is described by a nonlinear (exponential) relationship with respect to the volume fraction of ice (Calonne et al., 2011), so that a small amount of ice connecting ice grains has a strong impact on conductivity. Due to its lower thermal conductivity, this is not true for water, and a change of water content in the snow microstructure only causes a linear change in snow thermal conductivity. In the revised version, we included an analytical model of the unsaturated thermal conductivity (the self-consistent estimate of thermal conductivity for a 3-phase composite aggregate of spherical inclusions), which reproduces well the linear relationship between water content and snow thermal conductivity (see Fig. 3).

RECOMMENDATION

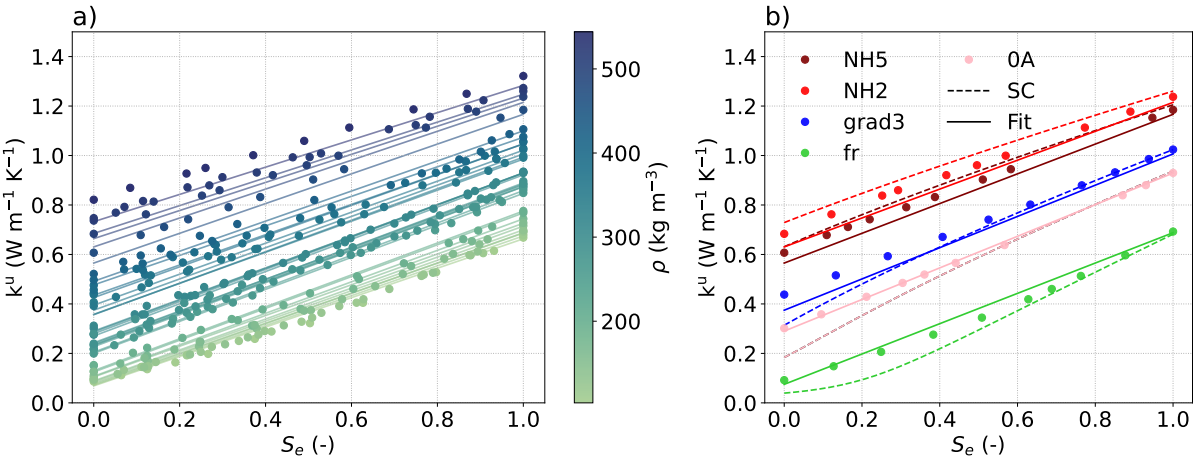

Figure 3. Unsaturated thermal conductivity k^u as a function of the effective saturation for (a) the whole set of snow samples, and (b) the 5 selected samples. Computations were performed on the snow images from the drainage simulations only. The dry density of the snow samples is represented by the colorbar. The suggested regression is shown by solid lines and the self-consistent estimate for 3 phases is shown by dashed lines.

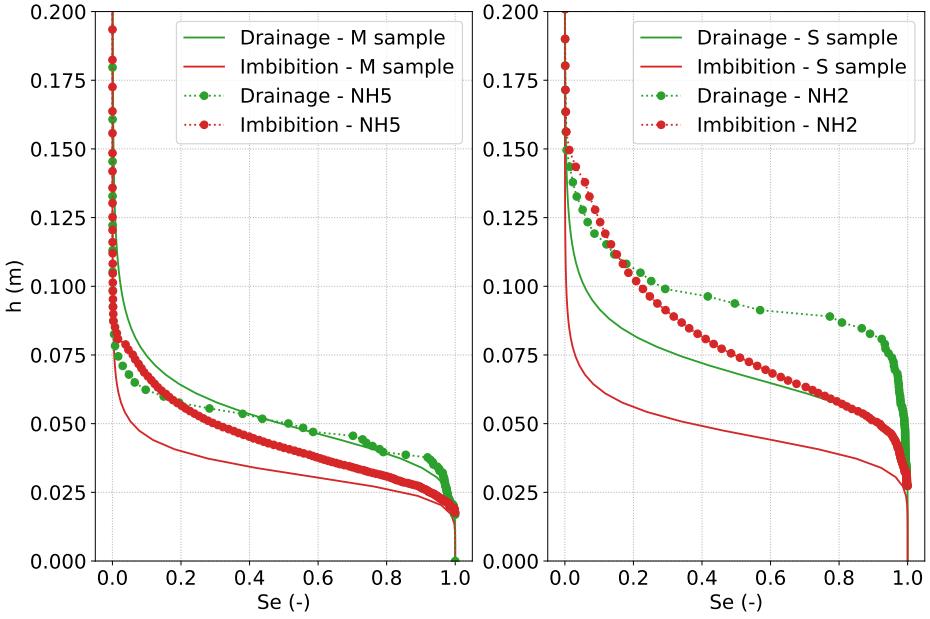

Figure 4. Comparison between drainage and imbibition experimental WRCs of M and S samples from Adachi et al. (2020) (solid curves) and the numerical estimates of NH2 and NH5 samples (dots and dotted lines).

I propose that the authors compare their model with experimental data as follows: Adachi et al. (2020) plotted in Figure 6 measured drainage and wetting curves of three snow samples ("S", "M", and "L"). According to Table 1 in Adachi et al. (2020), the dry snow densities were around 500 kg/m^3 and the snow particle diameter was 1.2 and 1.9 mm for the two finer snow samples ("S" and "M"). Considering that the samples of Adachi et al. (2020) are melted forms (but refrozen) and that two of your 'melted form samples' ("NH2" and "NH5") have similar densities and snow particle sizes as in Adachi et al., it would be meaningful to compare samples "S" and "M" with "NH2" and "NH5", respectively. With such comparison, you may show that the prediction of the drainage curve is close to the experimental values (I doubt a bit that the prediction of the wetting is successful too).

As recommended by the reviewer, Figure 4 presents a comparison between the WRCs from the M and S samples of Adachi et al. (2020) and our numerical estimates of WRCs for the melt forms samples NH5 and NH2. Having both experimental and simulation results on the same plot is interesting but not easy to compare, as they do not come from the same snow samples, although we picked up the closest samples in terms of snow types. We can see some similarities, such as the drainage curve aspects, even if a large vertical shift is found for NH2. Considerable differences can also be observed, such as the slope of the imbibition curves. It is, however, difficult to impute those differences on either the differences of snow sample (i.e. snow microstructure), on the numerical estimations, or on the experimental conditions. Such direct comparison would be more meaningful by comparing WRCs simulated and measured on the exact same sample. In the paper, we compare simulations versus experiments in terms of the shape parameters of the VG model and comment on the overall trends. For further assessment of our simulations, additional comparisons have been included, with Lombardo et al. (2025) and Katsushima et al. (2013), in the revised manuscript.

After such experimental proof, the authors could relate the simulated properties to various metrics of the pore space. In the present version, the authors consider the mean curvature but there are other properties of the pore space that should be considered (maximum and width of pore size distribution, and connectivity of the pore space as for example quantified by the Euler-Poincarè-characteristics). After such more detailed quantification of the imaged pore space, new relations between pore space characteristics and transport properties could be deduced with more confidence. You could also consider to fit the 'tortuosity parameter' in the Mualem van Genuchten expression of hydraulic conductivity (now set to ½) to see if it changes with snow structure.

We agree that other parameters related to pore space might, potentially, give interesting correlations. However, we tried many of them without any successful results. Concerning some particular metrics recommended, we presently have no access to any efficient numerical tool to confidently characterize these quantities. The mean curvature distribution is an effective way to access size distributions (e.g. Lesaffre et al. (1998), Calonne et al. (2014)), which give good results on our dataset. In addition, we think the mean curvature distribution is a parameter of choice for drainage and imbibition phenomena as it is directly related to the capillary pressure through the Laplace equation (see also the response to RC2 on this topic). In the revised manuscript, we improved our characterization of pore size uniformity by taking the interquartile range (IQR) of the mean curvature distribution instead of the standard deviation. It provides better results, as the IQR is more suited to the shape of our distributions (not always Gaussian) than the standard deviation.

Concerning the tortuosity parameter that can be included in the Mualem van Genuchten expression of hydraulic conductivity, at this stage, we use the common value 1/2. Its evolution with the snow microstructure will be studied in further works. This point is mention in the revised version of the manuscript

I propose to show the figures on the relationship between water content and capillary pressure using a linear scale of the pressure head, focusing on small absolute capillary pressure values. This allows a better assessment of the shape of the saturation-pressure relationship.

We agree with the reviewer and modified our figures accordingly, using linear pressure scales.

I suggest that the authors also show some cross-sections of the modeled phase distribution (similar to the mean curvature now shown in SI). This would facilitate to assess if the phase distribution is reasonable.

We agree with the reviewer. A new figure was made showing cross-sections of the 5 main images at 3 stages of the drainage and imbibition processes (Fig. 5). We added this figure to the manuscript in the subsection "WRCs of different snow microstructures and their related VG fits" with the corresponding description: "Figure 2 presents vertical cross-sections of the drainage and imbibition simulations at three stages of water saturation for the five selected snow samples described in Table 1. The pore-scale distribution of liquid water in the microstructures can be observed. For imbibition, the small pores are first filled, and the larger pores are filled last. For drainage, it is the other way around, with water escaping the large pore first. Residual liquid water at the end of the drainage simulation is shown in pink. Air bubbles entrapped in the ice skeleton are shown in yellow (for instance, in the bottom right of the 0A sample). This figure also highlights the fact that, for a given saturation, the liquid water distribution is different depending on the snow types, as well as between the imbibition and drainage processes."

The authors should also provide more information on the morphological pore network model.

The description of the pore morphology model (PMM) was significantly improved in the revised version in Section 2.3. It includes now: "The PMM uses a sphere with a radius r as a probe to detect the pore space that is accessible by the non-wetting phase (NWP, here the air). This radius is computed from the Young–Laplace equation: $r = 2\gamma\cos(\psi)/p_c$ where p_c is the capillary pressure, γ is the surface tension and ψ is the contact angle between ice and liquid water. At 0°C, γ = 0.0756 N m^{-1} and $\psi = 12°$ (Knight, 1967). Morphological operations, namely, erosion and /or dilation are used in the PMM (Hilpert and Miller, 2001). The algorithm of the PMM can be decomposed into several steps as follows:

- In drainage condition, the porous medium is initially saturated with the wetting phase (WP, here the water) (p_c = 0). The invading NWP is connected to the inlet, which is the NWP reservoir, and the WP can escape through the outlet, the WP reservoir. (i) Then, p_c is increased incrementally, i.e. r is decreased incrementally. The solid phase is first dilated by a sphere with radius r. (ii) All the pores connected to the NWP reservoir are labeled as NWP. (iii) The NWP is then dilated with the same sphere with radius r. The remaining pores are filled with the WP. The saturation can then be calculated. (iv) All the pores filled by the WP disconnected from the WP reservoir are considered as WP residual, and are no longer considered in the next steps. All these steps (i to iv) are repeated by increasing the value of the pressure, i.e. by decreasing the value of r. In the present case, the radius r was decreased gradually with a step of 2 pixel size.

- In imbibition condition, the porous medium is initially saturated with the NWP. The invading WP is connected to the inlet, which is the WP reservoir, and the NWP can escape through the outlet, the NWP reservoir. (i) Then, p_c is decreased incrementally, i.e. r is increased incrementally. The solid phase is first dilated by a sphere with radius r. (ii) The NWP is then dilated with the same sphere with radius r. (iii) All the pores connected to the WP are now labelled as WP. The remaining pores are NWP. The saturation can then be calculated. (iv) All the pores filled by the NWP disconnected from the NWP reservoir are considered as NWP residual, and are no longer considered in the next steps. As for the drainage condition, all these steps (i to iv) are repeated for the next value of the pressure, i.e. the next value of r. In the present case, the radius r was increased gradually with a step of 2 pixel size.

In the present study, the PMM implemented in the SatudDict software was used to compute the WRCs of the 34 snow samples. We computed (i) a primary imbibition curve assuming that there is no air (NWP) residuals as in MICP experiments, thus $\theta_w^s = \phi$ in Eq. 9, and then (ii) a primary drainage curve until to reach the water (WP) residuals (θ_w^r in Eq. 9). In both cases, symmetric boundary conditions are applied on the four sides of the volumes. The series of 3D snow images at different stages of drainage were then used to compute the relative permeability (i.e. the unsaturated hydraulic conductivity), the effective thermal conductivity, and the effective water vapor diffusivity.

Specific comments

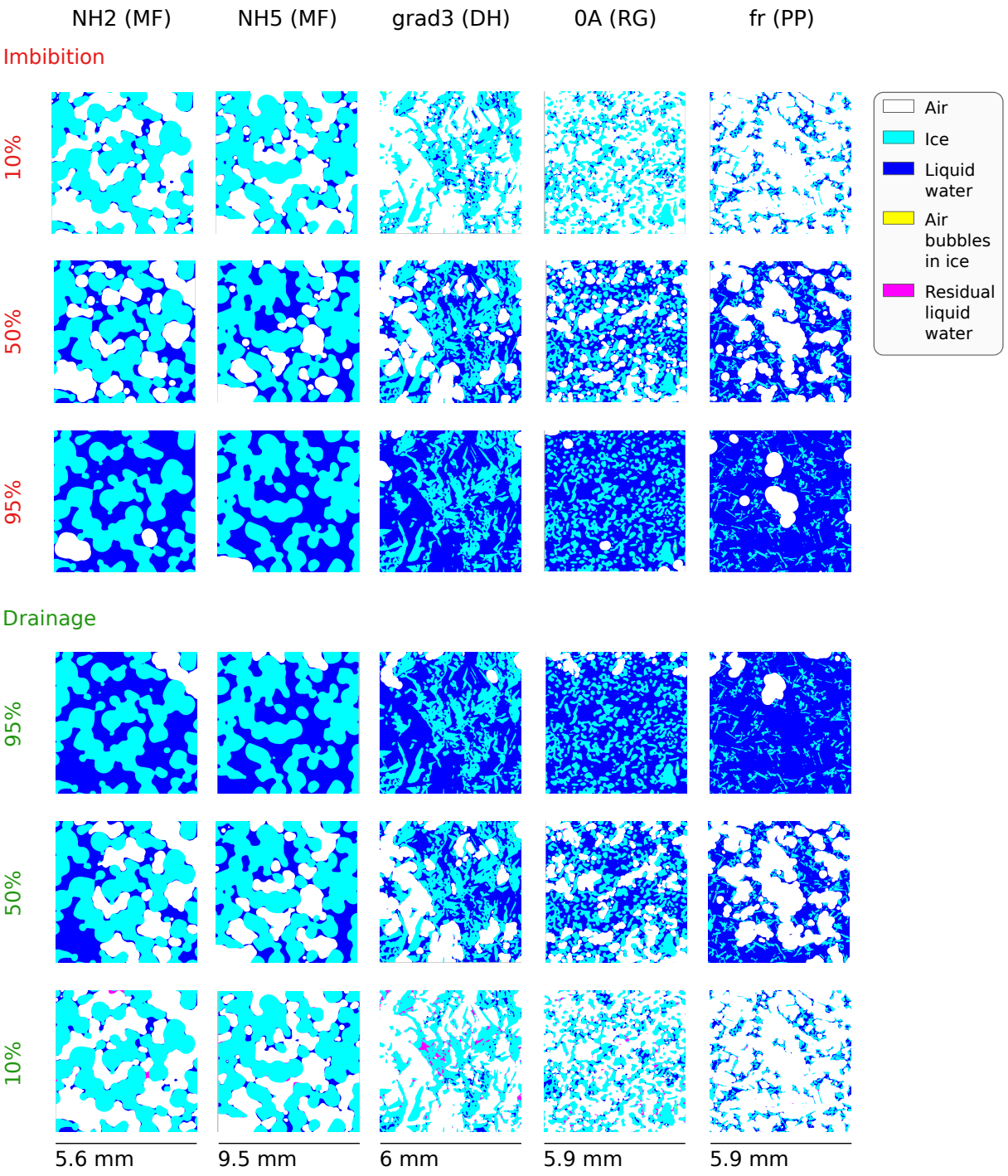

Figure 5. Vertical cross-sections of the 5 images with drainage and imbibition processes at 3 stages of effective saturation. The cross-sections are taken in the center of the samples. The reservoir of the wetting phase is located on the bottom boundary and the reservoir of the non-wetting phase is located on the top boundary.

Line 6: The term "time series" does not fit entirely, because temporal aspects are not considered.
The sentence was rephrased as: 'A series of wet snow images at different stages of drainage and imbibition, with different water contents, was produced.'

Line 39: I would write "shape parameters", not "hydraulic parameters".
The manuscript was modified accordingly.

Lines 42: There are other lab methods (evaporation method and dew point methods for dry soils.
The manuscript was modified accordingly.

Line 53: I think that in Yamaguchi et al. (2012) there are 12 samples that are not melted forms ("rounded grains" in Table 1).
We agree and corrected the description of the samples of Yamaguchi et al. (2012) in the introduction. It now reads 'The measurements of Yamaguchi et al. (2012) are the most extensive, based on 60 snow samples, yet restricted to sieved or natural melt forms and natural rounded grains, with high density values from 360 to 630 kg m^{-3}, and grain size from 0.3 to 5.8 mm.'

Line 56: Richards equation, not Richard equations.
The manuscript was modified accordingly.

Line 115: I found no specific information on the morphological pore network model in that paper.
The reference was removed (wrongly used).

Line 124: I propose to refer to the Young-Laplace equation because gravity is not included in the model (but the applied pressure)
The equation was changed to the Young-Laplace equation.

Lines 128-129: The text "The evolution of the air and liquid water in the ice structure can be seen as a series of erosion and dilation operations that depends on the pore distribution (Ahrenholz et al., 2008)" does not fit here -> erosion and dilation can be used to determine the pore size in complex structure but the evolution of the fluid phases is controlled by the connectivity as well.
We agree with the reviewer. As described in the above reply to the recommendation, the description of the pore morphology model used was significantly improved in section 2.3 of the revised version of the manuscript and this sentence was deleted

Line 131: How is it possible to reach saturation when air will be entrapped (and there must be air entrapment)?
As described in a dedicated comment above, residual air was not simulated and the saturation water content was set to equal the porosity.

Figure 2 : Write in the captions the name of the sample. Is there a melt form sample with such a high porosity?
Modified accordingly. The name of the snow sample was included in the caption.

Line 144: Why the "initial" liquid water? The connectivity of the liquid phase must be tested for each drainage step.
We agree with reviewer. The description of the pore morphology model used was significantly improved in section 2.3 of the revised version of the manuscript and takes into account this point.

Line 148: Have you tested the REV for the porosity? How is the porosity changing with image size?
The REV of the porosity for different types of snow has been investigated in Coléou et al. (2001), showing that most of the times the minimum REV is cubes with side of size 2 mm, which confirms that all our snow samples are larger than the REV for porosity.

Figure 3: this figure is "basic textbook" and is not needed here; please provide always the units of alpha.
The figure has been modified accordingly and the unit of α_{vg} was included. We think the figure is useful to make these concepts accessible to the snow community.

Line 166: it is the inverse of alpha that is related to the inflection point.
Modified accordingly.

Line 167: it is the "width" of the pore size distribution that controls the value of parameter "n".
Modified accordingly.

Lines 168/169: this is not correct considering the presence of entrapped air.
We did not simulate entrapped air. The lack of entrapped air in our simulations is addressed in a specific point above.

Line 169: state that the porosity can be deduced from dry bulk density and the density of ice.
Modified accordingly. The link between snow density and snow porosity is now presented in Section 2.2 of the manuscript.

Line 229: I am not sure that the smooth shape of the wetting curve is realistic.
The comment on the shape of our simulated WRCs is addressed in a specific point above.

Figure 6b: I cannot see the drainage regression line.
Given the observed scatter, no regression of the n parameter was provided as a function of ρ/d. However, regressions based on the mean curvature are provided, and are shown here in Figure 6.

Line 239: The exponential trend is not obvious because you have not enough values on the left side of the x-axis compared to Yamaguchi et al. (2012); in your data, there is a single sample with a x-value around 250000 kg/m^4; and a linear fit is almost as good as the exponential one for x-values $\geq$250000 kg/m^4.
We agree and deleted the term 'exponential' to describe the relationship of our simulated α parameter with ρ/d. We still used an exponential regression for α to be consistent with the regression form presented by Yamaguchi et al. (2012).

Line 259 : the differences in the findings of Yamaguchi et al. (2012) as function of snow type is important; but in your study you have also a few melted forms; have you checked if you find a trend in your melted-form-subset similar to Yamaguchi?
The n_{vg} values estimated for our five MF samples are further away from the regression of Yamaguchi et al. (2012) than the n_{vg} of Yamaguchi et al. (2012) measured on their MF samples (S samples and MF types from the N samples). The n_{vg} values estimated for our other snow types (RG, DF, PP and DH) are even more further away from the regression of Yamaguchi et al. (2012), which is consistent with the fact that the regression of Yamaguchi et al. (2012) was developed based on melt forms samples mostly. A sentence was included in the revised manuscript to highlight this effect: "Our estimated n_{vg} values for drainage overall do not follow the regression of Yamaguchi et al. (2012), even if the n_{vg} values of the melt form samples are closer to the regression compared to the other snow types.".

Lines 262 : To characterize the pore size variation, why don't you use the pore size distribution of the scanned sample? You should have access to the imaged pore size distribution (it is used as basis of the pore network model) and you could easily compute its width. This would be a more direct link to pore sizes compared to the curvature.
We tried several parameters in order to correlate the evolution of the VG model with the microstructure. The interquartile range of the curvature distributions appears to be the best one in that case, as described in the dedicated comment above.

Line 272 and Figure 7: the correlation is rather weak, and the nonlinearity is not very strong (similar correlation values for a linear fit); please explain colors in Figure 7.
Thank you for pointing that out. The linear fit is simpler and similar in terms of R2 (0.15 compared to 0.26 for the nonlinear fit) and MAE (2.5 compared to 2.3). However, our choice of regression is also motivated by the bounds of the function: the infinite bound of n_{vg} corresponds to the step WRC function that would be obtained with uniform pore sizes, and an asymptote value of n_{vg} for large values of σ_{MC} seems better than the negative values that would be obtained with a linear fit.

Line 283: this is an interesting result.

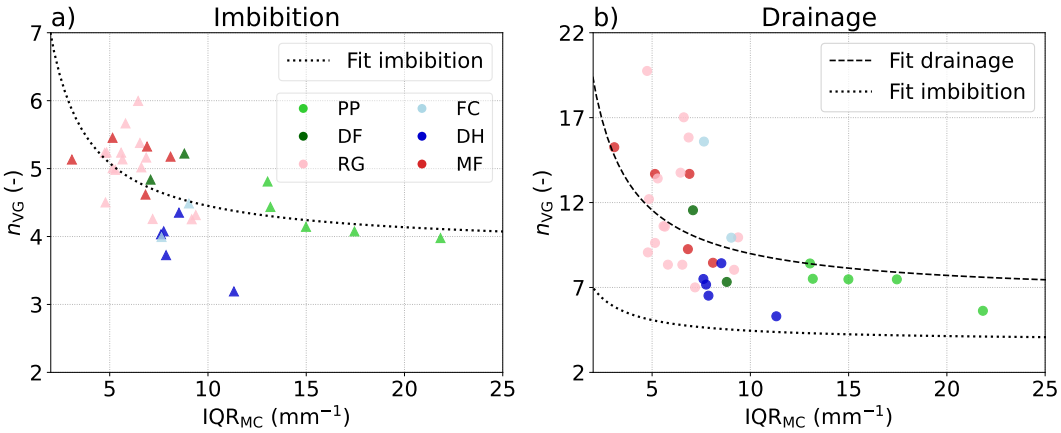

Figure 6. n_{vg} parameter as a function of the interquartile range IQR_{MC} obtained for the mean curvature distribution computed on each 3D dry snow image. Regressions for imbibition and drainage are shown with dotted and dashed lines.

Lines 286/287 : again-> I don't think that this is reasonable.

As already mentioned, we did not simulate residual air during imbibition, which indeed constitutes a simplification of the process. This point was clarified in the revised version of the manuscript.

Lines 303/304: The correlation with the standard deviation of mean curvature is rather weak and such regression may result in large prediction errors.

We improved our characterization of the pore size distribution by taking the interquartile range of the mean curvature distribution, instead of the standard deviation, as the distributions of mean curvature do not always correspond to a Gaussian shape. As seen in Figure 6, it enables to describe both n_{vg} for imbibition and drainage with the same inverse function, with standard deviations corresponding to: $(3.8 \pm 0.3) + (3.6 \pm 1.7)/\mathrm{IQR_{MC}}$ for imbibition and $(6.4 \pm 1.6) + (25.6 \pm 10.3)/\mathrm{IQR_{MC}}$ for drainage.

Line 314: Can you comment on the effect of applying different methods for the quantification of grain size?

The grain diameter estimation of Yamaguchi et al. (2012) slightly differs from ours: our definition is based on 3D snow images, whereas Yamaguchi et al.'s is based on its 2D counterpart obtained from outlines of disconnected ice grains. While the conceptual definition is quite similar for both of the methods, in which an "equivalent diameter" is estimated, some typical differences between 2D and 3D are well-documented (e.g Brzoska et al. (1999), Cooperdock et al. (2019)):

- The 2D method tends to neglect all snow structures related to necks between large disconnected grains;
- Due to the combination of gravity and projective effects, grain diameters may appear different in 2D than they really are in 3D;
- Tiny air bubbles or holes inside ice structures are often overlooked in 2D outlines.

Depending on grain types and specific morphologies, these methodological differences may result in an overestimation or an underestimation in grain sizes, so that an exact conversion between the two approaches cannot be reasonably achieved. As a consequence, comparing our results to those of Yamaguchi et al. (2012) in Fig 7 should be done by keeping in mind that estimation errors on the ρ/d values might exist, potentially as systematic errors (stretching of regression curves to the right or to the left) or as an increased dispersion of the dataset. Based on existing literature comparisons (e.g Brzoska et al. (1999), Cooperdock et al. (2019)), and on the figures obtained here (number and diversity of investigated snow samples and morphologies), we are quite confident that such errors are moderate and that overall comparisons between regressions obtained from the different methodologies are valid. Precise comparisons are, however,

more difficult and the difference between the regression of Yamaguchi et al. (2012) and our regression for α_{vg} in drainage could be e.g. interpreted as a consequence of this methodology difference. In this regard, our regression can be seen as an updated version of Yamaguchi et al. (2012)'s regression, proposing estimations that are based on systematic 3D diameter estimations, which are well adapted to tomographic measurements. The above explanations were added in the "3.1.3 Analysis of the VG parameters" subsection.

Figure 8a and 8b: please use the same intervals on x axis (0.1).
Modified accordingly.

Figure 8: why do the Yamaguchi curves have the same maximum saturation? I thought they used the 90% rule as maximum water content.
To ease the reading of the different models, and their different maximum water saturation, we plotted the WRCs as a function of the effective saturation instead of the water content.

Line 317: I do not agree with this conclusion considering the shape of the wetting curve, the lack of entrapped air in the model, and not enough samples to proof the non-linearity for small rho/d-values (smaller than 250'000 kg/m^4).
The comment on the shape of our simulated WRCs and the lack of entrapped air is addressed in a specific point above. We agree that we lack more samples to confirm the exponential decrease of the α parameter with rho/d, as in the data of Yamaguchi et al. (2012). We still used an exponential regression to be consistent with the regression form presented by Yamaguchi et al. (2012).

Lines 322/322: the new VG-model reproduces well the simulated values - but it is not clear that the simulations are correct.
This section was fully revised so that we now compare the VG model proposed in Yamaguchi et al. (2012), in Yamaguchi et al. (2012), in Daanen and Nieber (2009), without basing it on a comparison with the simulated WRCs on our snow samples, but based on a more independent approach. Indeed, instead of doing a comparison based on our snow samples, we defined two 'imaginary' snow samples. The properties of those samples have been chosen to be representative of melt forms (sample 1: d = 1.5 mm, ρ = 450 kg m^{-3}, IQR$_{\mathrm{MC}}$ = 5 mm^{-1}) and precipitation particles (sample 2: d = 0.1 mm, ρ = 130 kg m^{-3}, IQR$_{\mathrm{MC}}$ = 15 mm^{-1}). The section was renamed 'Application of the different VG models on two representative snow samples'.

Figure 10: I'm surprised that there are some samples with conductivity values of 10cm/day at effective water saturation of 0. How can this be? Do you have water flow along the residual water?
Thank you for pointing that out. Those points correspond to numerical artifacts that we had on a few images and have been removed from the figure. At this saturation, the liquid water phase is not connected from top to bottom, thus $\mathbb{K}_w^{\mathrm{u}} = 0$ m s^{-1}.

Equation 8 (and figures 10): you use the 'standard expression' with tortuosity factor "tau" of 1/2. This is an average value and can change with the porous medium (as discussed in Mualem 1976)
We added the definition of the tortuosity factor in the method section: "The exponent τ_{vg} describes the effects of the connectivity and tortuosity of the flow paths and is set to $1/2$, which is its default value (e.g., Mualem, 1976; Vereecken et al., 2010)." We also addressed this approximation in the section "Main limitations" that reads: "we chose a simple parameterization of the VG formulation, which can be refined using more parameters such as m_{vg} and τ_{vg} (see eq. 2 and 11)."

Line 343: the good agreement between the simulations and the 'standard formulation' of the Mualem-van Genuchten framework is no strong proof that the simulations are correct. You may try to fit the factor "tau" in Mualem van Genuchten for the different samples and check if the value changes with snow property.
Concerning the tortuosity parameter that can be included in the Mualem van Genuchten expression of hydraulic conductivity, at this stage, we use the common value 1/2. Its evolution with the snow microstructure will be studied in further work. This point is mentioned in the revised version of the manuscript.

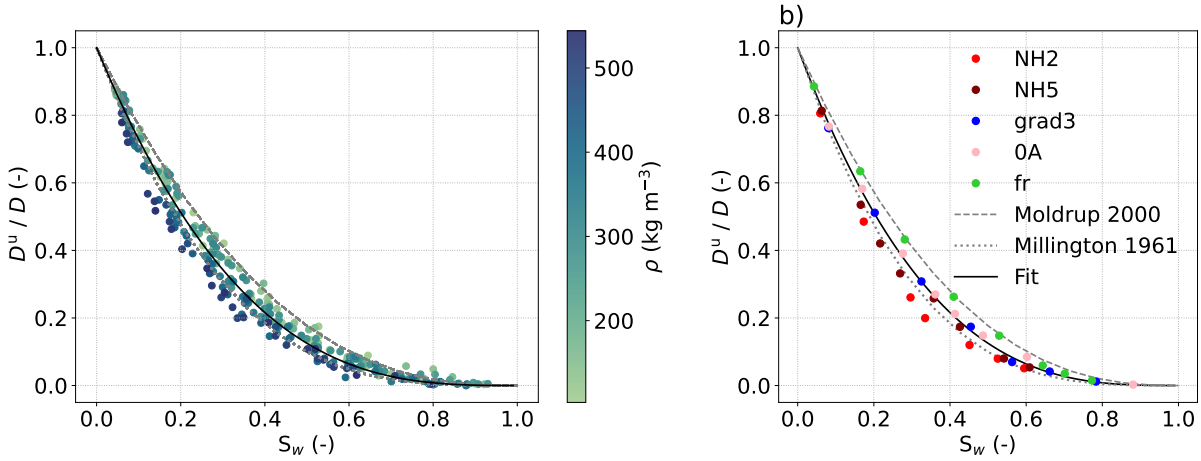

Figure 7. Relative water vapor diffusivity D^u/D as a function of the liquid water saturation S_w for drainage simulations of (a) the whole set of snow samples and (b) the 5 selected samples. The dry density of the snow samples is given by the colorbar. The proposed regression of unsaturated diffusivity is shown by a black solid line, and the models of Millington and Quirk (1961) and Moldrup et al. (2000) are shown with gray dotted and dashed lines respectively.

Figure 11: What are the predictions when you compute it without residual water? Maybe it is better to plot it as function of water content, not effective saturation.

Estimates of the thermal conductivity of snow without residual water, so for fully dry snow, can be found in Calonne et al. (2011), as we used the same set of dry snow images. Values for dry snow range from 0.06 W m^{-1} K^{-1} for a snow sample of density of 103 kg m^{-3} and 0.77 W m^{-1} K^{-1} for a snow sample of density of 544 kg m^{-3}.

Line 386: how do you know that it is over-estimated?

The thermal conductivity estimated in the Crocus model (Eq.14) is higher than the simulated thermal conductivity on 3D images of snow, as shown in Figure 12, and the higher the water content, the larger the difference. The Crocus model applies the same thermal conductivity-density relationship, regardless of the proportion of ice and liquid water, using the regression from Yen (1981) developed for dry snow. However, water conducts heat four times less than ice, which explains the overestimation.

Line 407/408: That is an interesting finding (similar approaches exist for gas diffusion in soils).

Line 414 : you should compare this with other models like Moldrup et al. (2000).

Following this remark, we added two models for D^u in unsaturated soils: the model of Millington and Quirk (1961) and of Moldrup et al. (2000). Both models are in good agreement with the numerical estimate and show similar relationships to our regression, bounding our regression with slightly higher and lower values, respectively. This comparison is now included in the revised version of the manuscript with Fig. 7 and a comment in the text : "This relationship follow the general form of estimates of $D^u/D_{dry} = (1 - \theta_w/\phi)^a$ classically used for soils (Kristensen et al., 2010) with $a = 10/3$ in Millington and Quirk (1961) and $a = 5/2$ in Moldrup et al. (2000). The regression is shown in Fig. 7 by the black line, along with the soil models of Millington and Quirk (1961) and Moldrup et al. (2000) that are displayed with gray dotted and dashed lines. The latter two models fairly represent the behavior of D^u and bound the regression for snow with higher and lower values. Both are used for predicting D^u in structureless natural soils."

Line 429: you should state this in the captions of figures 10-14.

The revised manuscript was modified accordingly.

Line 441: the pore size was not presented in this study.

We replaced 'pore size' by 'mean curvature distribution'.

References

Adachi, S., Yamaguchi, S., Ozeki, T., and Kose, K.: Hysteresis in the water retention curve of snow measured using an MRI system, in: Proceedings to the 2012 International Snow Science Workshop, Anchorage, Alaska, vol. 485, https://arc.lib.montana.edu/snow-science/objects/issw-2012-918-922.pdf, 2012.

Adachi, S., Yamaguchi, S., Ozeki, T., and Kose, K.: Application of a magnetic resonance imaging method for nondestructive, three-dimensional, high-resolution measurement of the water content of wet snow samples, Frontiers in Earth Science, 8, https://doi.org/10.3389/feart.2020.00179, 2020.

Ahrenholz, B., Tölke, J., Lehmann, P., Peters, A., Kaestner, A., Krafczyk, M., and Durner, W.: Prediction of capillary hysteresis in a porous material using lattice-Boltzmann methods and comparison to experimental data and a morphological pore network model, Advances in Water Resources, 31, 1151–1173, https://doi.org/10.1016/j.advwatres.2008.03.009, 2008.

Berg, S., Rücker, M., Ott, H., Georgiadis, A., van der Linde, H., Enzmann, F., Kersten, M., Armstrong, R., de With, S., Becker, J., and Wiegmann, A.: Connected pathway relative permeability from pore-scale imaging of imbibition, Advances in Water Resources, 90, 24–35, https://doi.org/https://doi.org/10.1016/j.advwatres.2016.01.010, 2016.

Brzoska, J. B., Lesaffre, B., Coléou, C., Xu, K., and Pieritz, R. A.: Computation of 3D curvatures on a wet snow sample, Eur. Phys. J. AP, 7, 45–57, https://doi.org/10.1051/epjap:1999198, 1999.

Calonne, N., Flin, F., Morin, S., Lesaffre, B., Rolland du Roscoat, S., and Geindreau, C.: Numerical and experimental investigations of the effective thermal conductivity of snow, Geophys. Res. Lett., 38, L23 501, https://doi.org/10.1029/2011GL049234, 2011.

Calonne, N., Flin, F., Geindreau, C., Lesaffre, B., and Rolland du Roscoat, S.: Study of a temperature gradient metamorphism of snow from 3-D images: time evolution of microstructures, physical properties and their associated anisotropy, The Cryosphere, 8, 2255–2274, https://doi.org/10.5194/tc-8-2255-2014, 2014.

Cho, J. Y., Lee, H. M., Kim, J. H., Lee, W., and Lee, J. S.: Numerical simulation of gas-liquid transport in porous media using 3D color-gradient lattice Boltzmann method: trapped air and oxygen diffusion coefficient analysis, Engineering Applications of Computational Fluid Mechanics, 16, 177–195, https://doi.org/10.1080/19942060.2021.2008012, 2022.

Clayton, W. S.: Effects of pore scale dead-end air fingers on relative permeabilities for air sparging in soils, Water Resources Research, 35, 2909–2919, https://doi.org/10.1029/1999WR900202, 1999.

Coléou, C., Lesaffre, B., Brzoska, J.-B., Ludwig, W., and Boller, E.: Three-dimensional snow images by X-ray microtomography, Annals of Glaciology, 32, 75–81, https://doi.org/10.3189/172756401781819418, 2001.

Cooperdock, E. H. G., Ketcham, R. A., and Stockli, D. F.: Resolving the effects of 2-D versus 3-D grain measurements on apatite (U–Th) / He age data and reproducibility, Geochronology, 1, 17–41, https://doi.org/10.5194/gchron-1-17-2019, 2019.

Daanen, R. P. and Nieber, J. L.: Model for Coupled Liquid Water Flow and Heat Transport with Phase Change in a Snowpack, Journal of Cold Regions Engineering, 23, 43–68, https://doi.org/10.1061/(ASCE)0887-381X(2009)23:2(43), 2009.

Farooq, U., Gorczewska-Langner, W., and Szymkiewicz, A.: Water retention curves of sandy soils obtained from direct measurements, particle size distribution, and infiltration experiments, Vadose Zone Journal, 23, e20 364, https://doi.org/10.1002/vzj2.20364, 2024.

Galindo-Torres, S., Scheuermann, A., and Li, L.: Boundary effects on the Soil Water Characteristic Curves obtained from lattice Boltzmann simulations, Computers and Geotechnics, 71, 136–146, https://doi.org/https://doi.org/10.1016/j.compgeo.2015.09.008, 2016.

Katsushima, T., Yamaguchi, S., Kumakura, T., and Sato, A.: Experimental analysis of preferential flow in dry snowpack, Cold Regions Science and Technology, 85, 206–216, https://doi.org/10.1016/j.coldregions.2012.09.012, 2013.

Katsushima, T., Adachi, S., Yamaguchi, S., Ozeki, T., and Kumakura, T.: Nondestructive three-dimensional observations of flow finger and lateral flow development in dry snow using magnetic resonance imaging, Cold Regions Science and Technology, 170, 102 956, https://doi.org/10.1016/j.coldregions.2019.102956, 2020.

Knight, C. A.: The contact angle of water on ice, Journal of Colloid and Interface Science, 25, 280–284, https://doi.org/10.1016/0021-9797(67)90031-8, 1967.

Kristensen, A. H., Thorbjørn, A., Jensen, M. P., Pedersen, M., and Moldrup, P.: Gas-phase diffusivity and tortuosity of structured soils, Journal of Contaminant Hydrology, 115, 26–33, https://doi.org/10.1016/j.jconhyd.2010.03.003, 2010.

Lesaffre, B., Pougatch, E., and Martin, E.: Objective determination of snow-grain characteristics from images, Annals of Glaciology, 26, 112–118, https://doi.org/10.3189/1998AoG26-1-112-118, 1998.

Likos, W. J., Lu, N., and Godt, J. W.: Hysteresis and Uncertainty in Soil Water-Retention Curve Parameters, Journal of Geotechnical and Geoenvironmental Engineering, 140, 04013 050, https://doi.org/10.1061/(ASCE)GT.1943-5606.0001071, 2014.

Lombardo, M., Fees, A., Kaestner, A., van Herwijnen, A., Schweizer, J., and Lehmann, P.: Quantification of capillary rise dynamics in snow using neutron radiography, EGUsphere, 2025, 1–36, https://doi.org/10.5194/egusphere-2025-304, 2025.

Millington, R. and Quirk, J.: Permeability of porous solids, Transactions of the Faraday Society, 57, 1200–1207, https://doi.org/10.1039/TF9615701200, 1961.

Moldrup, P., Olesen, T., Schjønning, P., Yamaguchi, T., and Rolston, D. E.: Predicting the Gas Diffusion Coefficient in Undisturbed Soil from Soil Water Characteristics, Soil Science Society of America Journal, 64, 94–100, https://doi.org/10.2136/sssaj2000.64194x, 2000.

Mualem, Y.: A new model for predicting the hydraulic conductivity of unsaturated porous media, Water Resources Research, 12, 513–522, https://doi.org/10.1029/WR012i003p00513, 1976.

Vereecken, H., Weynants, M., Javaux, M., Pachepsky, Y., Schaap, M. G., and Genuchten, M. v.: Using Pedotransfer Functions to Estimate the van Genuchten–Mualem Soil Hydraulic Properties: A ReviewAll rights reserved. No part of this periodical may be reproduced or transmitted in any form or by any means, electronic or mechanical, including photocopying, recording, or any information storage and retrieval system, without permission in writing from the publisher., Vadose Zone Journal, 9, 795–820, https://doi.org/10.2136/vzj2010.0045, 2010.

Vogel, H.-J., Tölke, J., Schulz, V. P., Krafczyk, M., and Roth, K.: Comparison of a Lattice-Boltzmann Model, a Full-Morphology Model, and a Pore Network Model for Determining Capillary Pressure-Saturation Relationships, Vadose Zone Journal, 4, 380–388, https://doi.org/https://doi.org/10.2136/vzj2004.0114, 2005.

Yamaguchi, S., Watanabe, K., Katsushima, T., Sato, A., and Kumakura, T.: Dependence of the water retention curve of snow on snow characteristics, Annals of Glaciology, 53, 6–12, https://doi.org/10.3189/2012AoG61A001, 2012.

Yen, Y.-C.: Review of thermal properties of snow, ice, and sea ice, vol. 81, US Army, Corps of Engineers, Cold Regions Research and Engineering Laboratory, https://apps.dtic.mil/sti/pdfs/ADA103734.pdf, 1981.

Zhang, Q., Liang, M., Zhang, Y., Wang, D., Yang, J., Chen, Y., Tang, L., Pei, X., and Zhou, B.: Numerical Study of Side Boundary Effects in Pore-Scale Digital Rock Flow Simulations, Fluids, 10, https://doi.org/10.3390/fluids10120305, 2025.